arXiv:nucl-th/0205052v1 19 May 2002

Effective Lagrangian approach to the ω photoproduction near threshold

Alexander I. Titov*

Advanced Science Research Center,

JAERI, Tokai, Ibaraki, 319-1195 Japan†

T.-S. H. Lee

Physics Division, Argonne National Laboratory, Argonne, Illinois 60439, USA‡

Abstract

We apply the effective Lagrangian approach to investigate the role of the nucleon resonances in ω meson photoproduction at energies near the threshold. The non-resonant amplitudes are taken from the previous investigations at higher energies and consist of the pseudoscalar meson exchange and the nucleon Born terms. The resonant amplitudes are calculated from effective Lagrangians with the $N^* \to \gamma N$ and $N^* \to \omega N$ coupling constants fixed by the empirical helicity amplitudes and the vector meson dominance model. The contributions from the nucleon resonances are found to be significant in changing the differential cross sections in a wide interval of t and various spin observables. In particular, we suggest that a crucial test of our predictions can be made by measuring single and double spin asymmetries.

PACS numbers: PACS number(s): 13.88.+e, 13.60.Le, 14.20.Gk, 25.20.Lj

---

*Bogoliubov Laboratory of Theoretical Physics, JINR, Dubna 141980, Russia

†Electronic address: atitov@thsun1.jinr.ru

‡Electronic address: lee@theory.phy.anl.gov

I. INTRODUCTION

The study of the decays of a nucleon resonance (N^*) into a nucleon (N) and a vector meson ($V = \omega, \rho, \phi$) is closely related to several aspects of intermediate and high energy physics, ranging from resolving the so-called "missing" resonance problem [1] to estimating the medium modifications on the vector meson properties [2, 3, 4, 5]. Electromagnetic production of vector mesons is one of the most promising reactions to determine the $N^* \to NV$ couplings experimentally, e.g., at Thomas Jefferson National Accelerator Facility, ELSA-SAPHIR of Bonn, GRAAL of Grenoble, and LEPS of SPring-8. The ω meson photoproduction has some advantages because the non-resonant contribution to its total amplitude is much better understood as compared with the other vector mesons[6].

The role of the nucleon resonances in ω meson photoproduction at relatively large energy was studied by Zhao *et al.* [7, 8, 9], using the $\mathrm{SU}(6) \times \mathrm{O}(3)$ constituent quark model with an effective quark-meson interaction. By fitting the model parameters to the existing data, they found that the single polarization observables are sensitive to the nucleon resonances and the dominant contribution at $E_\gamma \simeq 1.7$ GeV comes from the "missing" $F_{15}(2000)$ resonance. A recent analysis[10] of ω photoproduction in the same energy region makes use of the constituent quark model [11, 12], which accounts for the configuration mixing due to the residual quark-quark interactions [13]. In [10] the dominant contributions are found to be from $N\frac{3}{2}^+(1910)$, a missing resonance, and $N\frac{3}{2}^-(1960)$, which is identified as the $D_{13}(2080)$ of the Particle Data Group(PDG) [14]. As a result, the predicted single polarizations are rather different from those of [7]. Hopefully, the data from near future will clarify the situation.

It would be important to extend these studies to the low energy region, $E_\gamma \sim 1.1 - 1.25$ GeV, close to the omega production threshold, where the well established three- and four-star nucleon resonances are expected to be important. Unfortunately neither the approach of Ref. [7], nor of Ref. [10] could be applied for this investigation. The first approach[7] does not include the configuration mixing. Therefore, the predicted low-lying N^* states, belonging to the $[^4\mathbf{8}, \mathbf{70}]$ representation, can not contribute to the resonance photo excitation on the proton target because of the Moorhouse selection rule. That is, the contributions from $S_{11}(1650)$, $D_{15}(1675)$, and $D_{13}(1700)$ resonances are strictly suppressed [15]. This contradicts with the experimental data [14], which, for example, shows that photo excitation helicity amplitude $A_p^{\frac{1}{2}}$ for $S_{11}(1650)$ resonance is finite and large. In general, one finds that the SU(6)×O(3) quark model without configuration mixing forbids or suppresses most of the low mass resonances.

While the second approach[10] makes use of the information from the constituent quark model with configuration mixing, the $N^* \to \omega N$ transition amplitudes for the low-lying N^*'s with mass less than 1.72 GeV are not available in Ref.[12]. To provide such information, some extensions of the $^3P_0$ model employed in Ref.[12] for predicting $N^* \to \omega N$ are necessary.

As a possible solution of the problems mentioned above, we will follow the previous studies of π [16, 17] and η-photoproduction [18] and apply the effective Lagrangian approach to also describe the N^* excitation. Our approach is similar to the recent work by Riska and Brown[19], but with several significant differences. They fix the $N^*N\omega(\rho)$ effective Lagrangians for the low mass resonances with $M_{N^*} \leq 1720$ MeV by using the matrix elements derived from the SU(6)×O(3) constituent quark model with no configuration mixing. For the reasons mentioned above, an extension of their approach to also define the effective Lagrangian for $N^* \to \gamma N$ coupling will be unrealistic because of the restriction of the SU(6)×O(3) quark model. Thus their model is not applicable to a consistent investigation using effective Lagrangian approach. In this work, we will start with the empirical $N^* \to \gamma N$ amplitudes and then predict the needed $N^* \to \omega N$ coupling constants by using the vector meson dominance assumption. This is similar to a recent work by Post and Mosel[20]. But we will use a fully covariant formulation and explore in more detail the consequesncies of this approach.

To proceed, we need to also consider non-resonant mechanisms. It is fairly well established that the ω meson photoproduction is dominated by diffractive processes at high energies and by the one-pion exchange and the standard nucleon Born terms at low energies. The diffractive part is associated with the Pomeron exchange. In the near threshold energy the Pomeron exchange contribution is negligible and can be safely neglected in this work.

The calculation of the one-pion exchange amplitude(Fig.1a) and the direct and crossed nucleon terms(Figs. 1b and 1c) has been recently revived in Refs.[6, 10]. In this work we use the parameters determined in Ref.[10] to evaluate these non-resonant amplitudes. Our focus is to construct effective Lagrangians for calculating the resonant amplitude shown in Fig. 1(d,e) and explore their consequences in determining various spin observables.

This paper is organized as follows. In Section II we define the kinematics and the non-resonant amplitudes. Formula for calculating various spin observables will also be introduced there. The effective Lagrangians for calculating the amplitudes due to the excitations of nucleon resonances will be presented in Section III. In Section IV we present results and predictions for future experimental tests. The summary is given in Section V.

II. KINEMATICS, NON-RESONANT AMPLITUDE AND OBSERVABLES

The scattering amplitude T of $\gamma p \rightarrow \omega p$ reaction is related to the S-matrix by

$$S_{fi} = \delta_{fi} - i(2\pi)^4 \delta^4(k + p - q - p')T_{fi}, \tag{1}$$

where k, q, p and p' denote the four-momenta of the incoming photon, outgoing ω, initial nucleon, and final nucleon respectively. The standard Mandelstam variables are defined as $t = (p-p')^2 = (q-k)^2$, $s \equiv W^2 = (p+k)^2$, and the ω production angle θ by $\cos\theta \equiv \mathbf{k}\cdot\mathbf{q}/|\mathbf{k}||\mathbf{q}|$. The scattering amplitude is written as

$$T_{fi} = \frac{I_{fi}}{(2\pi)^6 \sqrt{2E_\omega(\mathbf{q})\, 2|\mathbf{k}| 2E_N(\mathbf{p}) 2E_N(\mathbf{p}')}}, \tag{2}$$

where $E_\alpha(\mathbf{p}) = \sqrt{M_\alpha^2 + \mathbf{p}^2}$ with M_α denoting the mass of the particle α. The invariant amplitude has two components

$$I_{fi} = I_{fi}^{BG} + I_{fi}^{N^*}, \tag{3}$$

where the resonance excitation term $I_{fi}^{N^*}$ will be derived in Sect. III. The non-resonant (background) amplitude is

$$I_{fi}^{BG} = I_{fi}^{PS} + I_{fi}^{N}, \tag{4}$$

with I_{fi}^{PS}, and I_{fi}^{N} denoting the amplitudes due to the pseudoscalar (π, η) meson exchange(Fig.1a), and the direct and crossed nucleon terms(Figs.1b and 1c), respectively. We calculate I_{fi}^{PS} by using the following effective Lagrangians

$$\mathcal{L}_{\omega\gamma\varphi} = \frac{e}{M_\omega} g_{\omega\gamma\varphi} \epsilon^{\mu\nu\alpha\beta} \partial_\mu \omega_\nu \partial_\alpha A_\beta\, \varphi, \tag{5}$$

$$\mathcal{L}_{PS} = -ig_{\pi^0 NN} \bar{N} \gamma_5\, \tau_3\, N\, \pi^0 - ig_{\eta NN} \bar{N} \gamma_5\, N\, \eta, \tag{6}$$

where $\varphi = \pi^0, \eta$, and A_β is the photon field. We use $g_{\pi NN}/4\pi = 14$ and $g_{\eta NN}/4\pi = 0.99$ for the πNN and ηNN couplings, respectively. The ηNN coupling constant has some uncertainties, but our choice is within the range reported in literatures. The $\omega\gamma\phi$ coupling constants can be estimated from the decay widths of $\omega \to \gamma\pi$ and $\omega \to \gamma\eta$ [14]. This leads to $g_{\omega\gamma\pi} = 1.823$ and $g_{\omega\gamma\eta} = 0.416$. The φNN and $\omega\gamma\varphi$ vertices are regularized by the following form factors

$$F_{\varphi NN}(t) = \frac{\Lambda_\varphi^2 - M_\varphi^2}{\Lambda_\varphi^2 - t}, \qquad F_{\omega\gamma\varphi}(t) = \frac{{\Lambda_{\omega\gamma\varphi}}^2 - M_\varphi^2}{{\Lambda_{\omega\gamma\varphi}}^2 - t}. \tag{7}$$

We evaluate the direct and crossed nucleon terms by using the following interaction Lagrangians

$$\mathcal{L}_{\gamma NN} = -e\left(\bar{N}\gamma_\mu \frac{1+\tau_3}{2} N A^\mu - \frac{\kappa_N}{2M_N}\bar{N}\sigma^{\mu\nu} N \partial_\nu A_\mu\right), \tag{8}$$

$$\mathcal{L}_{\omega NN} = -g_{\omega NN}\left(\bar{N}\gamma_\mu N \omega^\mu - \frac{\kappa_\omega}{2M_N}\bar{N}\sigma^{\mu\nu} N \partial_\nu \omega_\mu\right), \tag{9}$$

with $\kappa_{p(n)} = 1.79(-1.91)$. For the coupling constants we use $g_{\omega NN} = 10.35$ and $\kappa_\omega = 0$, which are close to the values determined in a study[17] of pion photoproduction. We follow Ref.[22] to assume that the γNN and ωNN vertices in Figs.1b and 1c are regularized by the following form factor

$$F_B(r^2) = \frac{\Lambda_B^4}{\Lambda_N^4 + (r^2 - M_B^2)^2}, \tag{10}$$

where M_B and r are the mass and the four-momentum of the intermediate baryon state.

The values of cutoff parameters for the form factors Eqs.(7) and (10) have been determined in a study[10] of $\gamma p \to \omega p$ at higher energies. Here we use their values with $\Lambda_\pi = \Lambda_{\omega\gamma\pi}^\pi = 0.6$ GeV/c, $\Lambda_\eta = 1$ GeV/c, and $\Lambda_{\omega\gamma\eta} = 0.9$ GeV/c for Eq.(7), and $\Lambda_B = \Lambda_N = 0.5$ GeV for Eq.(10). They are comparable to the values used in the literature and are sufficient for the present investigation. Other forms of form factors, such as those proposed recently in Ref.[23], will not be considered in this work.

We calculate all observables in the center of mass system(c.m.s.). The differential cross section is related to the invariant amplitude by

$$\frac{d\sigma_{fi}}{dt} = \frac{1}{64\pi(W^2 - M_N^2)^2} \sum_{\lambda_i\lambda_f\lambda_\gamma\lambda_\omega} |I_{fi}|^2, \tag{11}$$

where $\lambda_i, \lambda_\gamma$ are the helicities of the incoming nucleon and photon, and $\lambda_f, \lambda_\omega$ are the helicities of the outgoing nucleon and ω meson. In this paper we will also investigate the single and double spin observables [24]. The considered single observables, vector beam (Σ_x), target (T_y) and recoil (P_y) asymmetries, are defined by

$$\Sigma_x \;=\; \frac{\mathrm{Tr}\left[I_{fi}\sigma^x_\gamma\, I^\dagger_{fi}\right]}{\mathrm{Tr}\left[I_{fi}\, I^\dagger_{fi}\right]} = \frac{d\sigma_\perp - d\sigma_\parallel}{d\sigma_{\mathrm{tot}}}, \tag{12}$$

$$T_y \;=\; \frac{\mathrm{Tr}\left[I_{fi}\sigma^y_N\, I^\dagger_{fi}\right]}{\mathrm{Tr}\left[I_{fi}\, I^\dagger_{fi}\right]} = \frac{d\sigma^{s^N_y=\frac{1}{2}} - d\sigma^{s^N_y=-\frac{1}{2}}}{d\sigma_{\mathrm{tot}}}, \tag{13}$$

$$P_y \;=\; \frac{\mathrm{Tr}\left[I_{fi}\, I^\dagger_{fi}\, \sigma^x_{N'}\right]}{\mathrm{Tr}\left[I_{fi}\, I^\dagger_{fi}\right]} = \frac{d\sigma^{s^{N'}_y=\frac{1}{2}} - d\sigma^{s^{N'}_y=-\frac{1}{2}}}{d\sigma_{\mathrm{tot}}}, \tag{14}$$

where the subscript $\perp$ ($\|$) corresponds to a photon linearly polarized along the $\mathbf{y}$ ($\mathbf{x}$) axis; $s^N_y = \frac{1}{2}\,(-\frac{1}{2})$ corresponds to the case that the proton polarization is parallel (antiparallel) to the $\mathbf{y}$ axis. At $\omega-$meson production angle $\theta = 0, \pi$, the amplitudes with the orbital momentum projection $m_l \neq 0$ vanish and the spin conserving argument results in

$$\Sigma_x = T_y = P_y = 0, \qquad\qquad \text{at } \theta = 0. \tag{15}$$

For the outgoing ω meson we consider tensor asymmetry

$$V_{z'z'} = \frac{\mathrm{Tr}\left[I_{fi}\, I^\dagger_{fi}\, S^{zz}_\omega\right]}{\mathrm{Tr}\left[I_{fi}\, I^\dagger_{fi}\right]} = \frac{d\sigma^{s^\omega_{z'}=1} + d\sigma^{s^\omega_{z'}=-1} - 2d\sigma^{s^\omega_{z'}=0}}{\sqrt{2}d\sigma_{\mathrm{tot}}}, \tag{16}$$

where S^{zz}_ω is the tensor polarization operator for a spin 1 particle [25] and s^ω_z is the ω meson spin projection along the quantization axis $\mathbf{z}'$. For the pseudoscalar π, η- exchange, which is the dominant non-resonant amplitude, the tensor polarization may be written in a compact form

$$V^{PS}_{z'z'} = \frac{3}{2\sqrt{2}}\left[\left(\frac{v_\omega - \cos\theta}{1 - v_\omega\cos\theta}\right)^2 - \frac{1}{3}\right], \tag{17}$$

where v_ω is the ω-meson velocity in c.m.s.. This expression shows that at $\theta = 0$, $V^{PS}_{z'z'} = 1/\sqrt{2}$. The asymmetry $V^{PS}_{z'z'}$ has the simplest form in the Gottfried-Jackson frame in which the ω-meson is at rest and the $\mathbf{z}$ axis is in the direction of the incoming photon momentum. In this frame the helicity conserving pseudoscalar exchange amplitude has a simple form

$$I^{PS}_{\lambda_\omega\lambda_\gamma} \sim \lambda_\gamma\delta_{\lambda_\omega\lambda_\gamma}, \tag{18}$$

which shows that the longitudinally polarized ω mesons are forbidden. As result, one get the asymmetry $V^{PS}_{z'z'}$ to be constant at all θ

$$V^{PS}_{z'z'} = \frac{1}{\sqrt{2}}. \tag{19}$$

A deviation from this pseudoscalar meson-exchange value will measure the contributions from other mechanisms. We will see that the contribution of other channels illustrated in Fig.1, especially at large θ, leads to deviation from this value.

We will also consider the beam-target double asymmetry, defined as

$$C^{BT}_{zz} = \frac{d\sigma(\uparrow\downarrow) - d\sigma(\uparrow\uparrow)}{d\sigma(\uparrow\downarrow) + d\sigma(\uparrow\uparrow)}, \tag{20}$$

where the arrows represent the helicities of the incoming photon and the target protons.

III. EXCITATION OF NUCLEON RESONANCES

For evaluating the resonant amplitude $I^{N^*_L}_{fi}$, we consider the isospin $I = 1/2$ nucleon resonances listed by PDG[14]. However only the resonances with the empirical helicity amplitudes of $\gamma N \to N^*$ transitions given by PDG can be included in our approach, as will be clear below. We thus have contributions from 12 resonances: $P_{11}(1440)$, $D_{13}(1520)$, $S_{11}(1535)$, $S_{11}(1650)$, $D_{15}(1675)$, $F_{15}(1680)$, $D_{13}(1700)$, $P_{11}(1710)$, $P_{13}(1720)$, $F_{17}(1990)$, $D_{13}(2080)$, and $G_{17}(2190)$. Our first task here is to define effective Lagrangians for reproducing the empirical helicity amplitudes for the $\gamma N \to N^*$ transitions for these resonances.

For the N^* with spin $J = \frac{1}{2}$, the effective Lagrangians for the γNN^* interactions are chosen to be of the form of the usual γNN interaction. But only the tensor coupling is kept, since the vector coupling violates the gauge invariance for the considered $M_{N^*} \neq M_N$ cases. This "minimal" form of Lagrangian, previously used in the study of η-photoproduction [18], is

$$\mathcal{L}^{\frac{1}{2}^{\pm}}_{\gamma NN^*} = \frac{eg_{\gamma NN^*}}{2M_{N^*}} \bar{\psi}_{N^*} \Gamma^{(\pm)} \sigma_{\mu\nu} F^{\mu\nu} \psi_N + \text{h.c.}, \tag{21}$$

where ψ_N, ψ_{N^*} and A_μ are the nucleon, nucleon resonance, and photon fields, respectively, and $F^{\mu\nu} = \partial^\nu A^\mu - \partial^\mu A^\nu$. The coupling $\Gamma^+ = 1(\Gamma^- = \gamma_5)$ defines the excitation of a positive(negative) parity N^* state.

For the N^* with spin $J = \frac{3}{2}$, we use the expression introduced in Refs. [16, 18, 26]

$$\mathcal{L}^{\frac{3}{2}^{\pm}}_{\gamma NN^*} = i\frac{eg_{\gamma NN^*}}{M_{N^*}}\bar{\psi}^{\mu}_{N^*}\, O_{\mu\nu}(Z)\gamma_{\lambda}\Gamma^{(\mp)}F^{\lambda\nu}\psi_N \qquad + \text{h.c.}, \tag{22}$$

where ψ_α is the Rarita-Schwinger spin-$\frac{3}{2}$ baryon field. The off-shell operator $O_{\mu\nu}(Z)$ is

$$O_{\mu\nu}(Z) = g_{\mu\nu} + \left[\frac{1}{2}(1+4Z)A + Z\right]\gamma_\mu\gamma_\nu, \tag{23}$$

where A is an arbitrary parameter, defining the so-called "point transformation". Since the the physical amplitudes are independent of A, we follow Ref.[18] to choose $A = -1$. When both N and N^* are on-mass-shell, Eq. (22) is equivalent to the form commonly used[27, 28] in the investigation of pion photoproduction.

The effective Lagrangians for the resonances with $J^P = \frac{5}{2}^{\pm}, \frac{7}{2}^{\pm}$ are constructed by the analogy with the previous case

$$\mathcal{L}^{\frac{5}{2}^{\pm}}_{\gamma NN^*} = \frac{eg_{\gamma NN^*}}{M^2_{N^*}}\bar{\psi}^{\mu\alpha}_{N^*}\, O_{\mu\nu}(Z)\gamma_{\lambda}\Gamma^{(\pm)}(\partial_\alpha F^{\lambda\nu})\psi_N \qquad + \text{h.c.}, \tag{24}$$

$$\mathcal{L}^{\frac{7}{2}^{\pm}}_{\gamma NN^*} = -i\frac{eg_{\gamma NN^*}}{M^3_{N^*}}\bar{\psi}^{\mu\alpha\beta}_{N^*}\, O_{\mu\nu}(Z)\gamma_{\lambda}\Gamma^{(\mp)}(\partial_\beta\partial_\alpha F^{\lambda\nu})\psi_N \qquad + \text{h.c.}, \tag{25}$$

where $\psi_{\alpha\beta}$, and $\psi_{\alpha\beta\gamma}$ are the Rarita-Schwinger spin $\frac{5}{2}$ and $\frac{7}{2}$ field, respectively. The interaction (24) is a covariant generalization of non-relativistic expression used in Ref. [2].

We define the ωNN^* coupling by using the vector dominance model (VDM). It amounts to assuming that the electromagnetic and vector meson fields are related to each other by

$$A^\mu_s = \frac{em^2_\omega}{2\gamma_\omega}\,\omega^\mu, \qquad A^\mu_v = \frac{em^2_\rho}{2\gamma_\rho}\,\rho^\mu, \tag{26}$$

where $A_{s(v)}$ is the isoscalar (isovector) part of electromagnetic field. The coupling strengths $\gamma_\omega = 8.53$ and $\gamma_\rho = 2.52$ are fixed by the electromagnetic $\omega \to e^+e^-$, $\rho \to e^+e^-$ decays [6]. In the VDM approach the effective $\mathcal{L}_{\omega NN^*}$ Lagrangian has the same form as the corresponding $\mathcal{L}_{\gamma NN^*}$ with substitution

$$A_\mu \to \omega_\mu, \qquad eg_{\gamma NN^*} \to f_\omega, \tag{27}$$

with

$$f_\omega = 2g_s\gamma_\omega. \tag{28}$$

The scalar coupling constant g_s is related to the strengths of the N^* excitations on the proton($g_p = g_{\gamma pN^*}$) and on the neutron($g_n = g_{\gamma nN^*}$)

$$g_s = \frac{g_p + g_n}{2}. \tag{29}$$

With the Lagrangians for γNN^* and ωNN^* couplings specified above, we can calculate the invariant amplitudes for the N^* excitation mechanisms illustrated in Figs. 1d and 1e. The resulting invariant amplitudes have the following form

$$I_{fi}^{(N^*)} = eg_{\gamma NN^*} f_{\omega NN^*} \bar{u}(p') \mathcal{A}^{\mu\nu}(N^*) u(p) \varepsilon_\mu^{\omega *} \varepsilon_\nu^{\gamma}, \tag{30}$$

where the operators $\mathcal{A}_{\mu\nu}$ are completely defined by the effective Lagrangians (21) - (24)

$$\mathcal{A}_{\mu\nu}^{\frac{1}{2}^\pm} = -\frac{eg_{\gamma NN^*} f_{\omega NN^*}}{M_{N^*}^2} \left[\gamma_\mu \not{q} \mathcal{P}^{s\pm}(N^*) \gamma_\nu \not{k} F_{N^*}(s) + \gamma_\nu \not{k} \mathcal{P}^{u\pm}(N^*) \gamma_\mu \not{q} F_{N^*}(u) \right], \tag{31}$$

$$\begin{aligned} \mathcal{A}_{\mu\nu}^{\frac{3}{2}^\pm} &= \mp \frac{eg_{\gamma NN^*} f_{\omega NN^*}}{(M_{N^*}^2} \Gamma^{(\mp)} \, [\, \overline{W}_\mu^\alpha \mathcal{P}_{\alpha\beta}^s(N^*) E_\nu^\beta F_{N^*}(s) \\ &\qquad + \overline{E}_\mu^\alpha \mathcal{P}_{\alpha\beta}^u(N^*) W_\nu^\beta F_{N^*}(u) \,] \; \Gamma^{(\mp)}, \end{aligned} \tag{32}$$

$$\begin{aligned} \mathcal{A}_{\mu\nu}^{\frac{5}{2}^\pm} &= \pm \frac{eg_{\gamma NN^*} f_{\omega NN^*}}{M_{N^*}^4} \Gamma^{(\pm)} \, [\, \overline{W}_\mu^\alpha q^{\alpha'} \mathcal{P}_{\alpha\alpha',\beta\beta'}^s(N^*) k^{\beta'} E_\nu^\beta F_{N^*}(s) \\ &\qquad + \overline{E}_\mu^\alpha k^{\alpha'} \mathcal{P}_{\alpha\alpha',\beta\beta'}^u(N^*) q^{\beta'} W_\nu^\beta F_{N^*}(u) \,] \, \Gamma^{(\pm)} \end{aligned} \tag{33}$$

$$\begin{aligned} \mathcal{A}_{\mu\nu}^{\frac{7}{2}^\pm} &= \mp \frac{eg_{\gamma NN^*} f_{\omega NN^*}}{M_{N^*}^6} \Gamma^{(\mp)} \, [\, \overline{W}_\mu^\alpha q^{\alpha'} q^{\alpha''} \mathcal{P}_{\alpha\alpha'\alpha'',\beta\beta'\beta''}^s(N^*) k^{\beta'} k^{\beta''} E_\nu^\beta F_{N^*}(s) \\ &\qquad + \overline{E}_\mu^\alpha k^{\alpha'} k^{\alpha''} \mathcal{P}_{\alpha\alpha'\alpha'',\beta\beta'\beta''}^u(N^*) q^{\beta'} q^{\beta''} W_\nu^\beta F_{N^*}(u) \,] \, \Gamma^{(\mp)} \end{aligned} \tag{34}$$

In the above equations, we have introduced

$$\begin{aligned} \overline{W}_\mu^\alpha &= (\not{q} g_{\mu\nu} - \gamma_\mu q_\nu) \, O^{\nu\alpha}(X), & \overline{E}_\mu^\alpha &= (\not{k} g_{\mu\nu} - \gamma_\mu k_\nu) \, O^{\nu\alpha}(X), \\ W_\mu^\alpha &= O^{\alpha\nu}(X) \, (\not{q} g_{\mu\nu} - \gamma_\mu q_\nu), & E_\mu^\alpha &= O^{\alpha\nu}(X) \, (\not{k} g_{\mu\nu} - \gamma_\mu k_\nu). \end{aligned} \tag{35}$$

The resonance propagators $\mathcal{P}(N^*)$ in Eqs.(31)-(34) are defined by making use of the conventional prescription [29] that the following spectral decomposition of the N^* field is valid

$$\psi_{N^*}(x) = \int \frac{d^3\mathbf{p}}{(2\pi)^3 \sqrt{2E_p}} \left[a_{\mathbf{p},r} \, u_{N^*}^r(p) e^{-ipx} + b_{\mathbf{p},r}^+ \, v_{N^*}^r(p) e^{+ipx} \right], \tag{36}$$

where u_{N^*}, v_{N^*} are the Rarita-Schwinger spinors. The finite decay width Γ_{N^*} is introduced into the denominators of the propagators by the substitution $M_{N^*} \rightarrow M_{N^*} - \frac{i}{2}\Gamma_{N^*}$. Explicitly, we then have for the $J = \frac{1}{2}$ case(Eq.(31))

$$\mathcal{P}^\pm(N^*) = \frac{\Lambda^\pm(p, M_{N^*})}{p_r^2 - M_{N^*}^2 + i\Gamma_{N^*} M_{N^*}}, \tag{37}$$

The the spin projection operators $\Lambda^{\pm}(p, M)$ in the above equation are defined by the bilinear combinations of the Rarita-Schinger spinors

$$\begin{aligned}
\Lambda^{+}(p, M) &= \frac{1}{2}\sum_{r}\Bigg((1+\frac{p_0}{E_0})u^r(\mathbf{p}, E_0)\otimes\bar{u}^r(\mathbf{p}, E_0) \\
&\qquad -(1-\frac{p_0}{E_0})v^r(-\mathbf{p}, E_0)\otimes\bar{v}^r(-\mathbf{p}, E_0)\Bigg) \\
&= \not{p} + M, \\
\Lambda^{-}(p, M) &= \not{p} - M
\end{aligned} \tag{38}$$

where $E_0 = \sqrt{\mathbf{p}^2 + M^2}$, u and v are the usual Dirac spinors. The projection operators P_{ab} with $a = \alpha, \alpha\beta, \alpha\beta\gamma$, in Eqs.(32) - (34) take the same form of Eq.(37), except that their projection operators have the following higher-rank tensor forms

$$\begin{aligned}
\Lambda_{\alpha\beta}(p, M) &= \frac{1}{2}\sum_{r}\Bigg((1+\frac{p_0}{E_0})\mathcal{U}^r_{\alpha}(\mathbf{p}, E_0)\otimes\bar{\mathcal{U}}^r_{\beta}(\mathbf{p}, E_0) \\
&\qquad -(1-\frac{p_0}{E_0})\mathcal{V}^r_{\alpha}(-\mathbf{p}, E_0)\otimes\bar{\mathcal{V}}^r_{\beta}(-\mathbf{p}, E_0)\Bigg)\,; \qquad (39) \\
\Lambda_{\alpha\beta,\gamma\delta}(p, M) &= \frac{1}{2}\sum_{r}\Bigg((1+\frac{p_0}{E_0})\mathcal{U}^r_{\alpha\beta}(\mathbf{p}, E_0)\otimes\bar{\mathcal{U}}^r_{\gamma\delta}(\mathbf{p}, E_0) \\
&\qquad -(1-\frac{p_0}{E_0})\mathcal{V}^r_{\alpha\beta}(-\mathbf{p}, E_0)\otimes\bar{\mathcal{V}}^r_{\gamma\delta}(-\mathbf{p}, E_0)\Bigg)\,, \qquad (40) \\
\Lambda_{\alpha\beta\gamma,\delta\sigma\xi}(p, M) &= \frac{1}{2}\sum_{r}\Bigg((1+\frac{p_0}{E_0})\mathcal{U}^r_{\alpha\beta\gamma}(\mathbf{p}, E_0)\otimes\bar{\mathcal{U}}^r_{\delta\sigma\xi}(\mathbf{p}, E_0) \\
&\qquad -(1-\frac{p_0}{E_0})\mathcal{V}^r_{\alpha\beta\gamma}(-\mathbf{p}, E_0)\otimes\bar{\mathcal{V}}^r_{\delta\sigma\xi}(-\mathbf{p}, E_0)\Bigg)\,, \qquad (41)
\end{aligned}$$

where the Rarita-Schwinger spinors are defined by

$$\begin{aligned}
\mathcal{U}^r_{\alpha}(p) &= \sum_{\lambda,s}\langle 1\,\lambda\,\frac{1}{2}\,s|\,\frac{3}{2}\,r\rangle\,\varepsilon^{\lambda}_{\alpha}(p)\,u^s(p), \\
\mathcal{U}^r_{\alpha\beta}(p) &= \sum_{\lambda,\lambda' s,t}\langle 1\,\lambda\,\frac{1}{2}\,s|\,\frac{3}{2}\,t\rangle\,\langle\frac{3}{2}\,t\,1\,\lambda'|\,\frac{5}{2}\,r\rangle\,\varepsilon^{\lambda}_{\alpha}(p)\,\varepsilon^{\lambda'}_{\beta}(p)\,u^s(p), \\
\mathcal{U}^r_{\alpha\beta\gamma}(p) &= \sum_{\lambda,\lambda',\lambda'',s,t,w}\langle 1\,\lambda\,\frac{1}{2}\,s|\,\frac{3}{2}\,t\rangle\,\langle\frac{3}{2}\,t\,1\,\lambda'|\,\frac{5}{2}\,w\rangle\,\langle\frac{5}{2}\,w\,1\,\lambda''|\,\frac{7}{2}\,r\rangle\,\varepsilon^{\lambda}_{\alpha}(p)\,\varepsilon^{\lambda'}_{\beta}(p)\,\varepsilon^{\lambda''}_{\gamma}(p)\,u^s(p)
\end{aligned} \tag{42}$$

The spinors v and $\mathcal{V}$ are related to u and $\mathcal{U}$ as $v(p) = i\gamma_2\, u^*(p)$ and $\mathcal{V}(p) = i\gamma_2\,\mathcal{U}^*(p)$, respectively. The polarization four-vector $\varepsilon^{\lambda}_{\mu}$ for a spin-1 particle with spin projection λ, four-momentum $p = (E, \mathbf{p})$ and mass m, is

$$\varepsilon^{\lambda}(p) = \left(\frac{\boldsymbol{\epsilon}^{\lambda}\cdot\mathbf{p}}{m},\ \boldsymbol{\epsilon}^{\lambda} + \frac{\mathbf{p}\,(\boldsymbol{\epsilon}^{\lambda}\cdot\mathbf{p})}{m(E+m)}\right), \tag{43}$$

where the three-dimensional polarization vector $\boldsymbol{\epsilon}$ is defined by

$$\boldsymbol{\epsilon}^{\pm 1} = \mp\frac{1}{\sqrt{2}}(\,1,\ \pm i,\ 0\,), \boldsymbol{\epsilon}^{0} = (\,0,\ 0,\ 1\,). \tag{44}$$

At first glance it seems that the spin projection operator Eq.(39) for $J = \frac{3}{2}$ N^* is rather different from the commonly used on-shell operator $\overline{\Lambda}_{\alpha\beta}(p, M)$, which may be obtained [30] from the Rarita-Schwinger spinors

$$\begin{aligned}\overline{\Lambda}_{\alpha\beta}(p, M) &= \sum_r \mathcal{U}^r_\alpha(\mathbf{p}) \otimes \bar{\mathcal{U}}^r_\beta(\mathbf{p}) \\ &= -\left[g_{\alpha\beta} - \frac{1}{3}\gamma_\alpha\gamma_\beta - \frac{\gamma_\alpha p_\beta - \gamma_\beta p_\alpha}{3M} - \frac{2p_\alpha p_\beta}{3M^2}\right](\not{p} + M). \end{aligned} \tag{45}$$

We now note that at the on-shell $p^2 = M^2$ point, the contribution from of the second terms in Eqs.(39) vanishes and $\Lambda_{\alpha\beta}(p, M) = \overline{\Lambda}_{\alpha\beta}(p, M)$.

There are some arbitrariness in defining the propagators of higher spin particles. In this work we use the prescription based on Eqs.(31)- (33) and Eqs.(38) - (40) because (i) it coincides at mass shell with the well known spin $\frac{3}{2}$ propagator Eq.(45) and (ii) it gives correct off-shell behavior for $\frac{1}{2}$ baryons. We remark that the form Eq.(45) for $J = \frac{3}{2}$ particles has some unphysical features for the off-shell $p^2 \neq M^2$ cases, which can not be fixed for both the s and u channel N^* excitations by making the simple substitution[39] $M \rightarrow \sqrt{p^2}$.

The effect of the finite resonance decay width is quite different for s and u channels, because of the evident relation $|u| + M^2_{N^*} \gg |s - M^2_{N^*}|$. Therefore, for simplicity, for the u channels we use a constant value $\Gamma_{N^*} = \Gamma^0_{N^*}$. For the s channels the energy-dependent widths are calculated according to Ref.[32]

$$\Gamma(W) = \sum_j \Gamma_j \frac{\rho_j(W)}{\rho_j(M_{N^*})}. \tag{46}$$

where Γ_j is the partial width for the resonance decay into the jth channel, evaluated at $W \equiv \sqrt{s} = M_{N^*}$. The form of the "space-phase" factor $\rho_j(W)$ depends on the decay channel, the relative momentum q_j of the outgoing particles, and their relative orbital momentum l_j. It provides proper analytic threshold behaviour $\rho_j(W) \sim q_j^{2l_j+1}$ as $q_j \rightarrow 0$ and becomes constant at high energy [33].

Our next task is to fix the coupling constants in the effective Lagrangians Eqs.(21),(22), (24), and (25). They can be calculated by using the empirical helicity amplitudes listed by Particle Data Group [14]. For the spin $J = \frac{1}{2}$ resonances we find that

$$eg_a = \pm\frac{C}{2\sqrt{2}k^*}\, A_a^{\frac{1}{2}}, \tag{47}$$

with

$$k^* = \frac{M_{N^*}^2 - M_N^2}{2M_{N^*}}, \qquad C = \sqrt{8M_N M_{N^*} k^*} \tag{48}$$

and $a = p, n, s$.

For spin $J = \frac{3}{2}, \frac{5}{2}, \frac{7}{2}$ particles, the relations between the helicity amplitudes and coupling constants are given by

$$J^P = \frac{3}{2}^{\pm}$$

$$eg_a = \pm\frac{\sqrt{3}C}{2M_N}\frac{M_{N^*}}{k^*}A_a^{\frac{1}{2}}, \qquad eg_a = \pm\frac{C}{2M_{N^*}}\frac{M_{N^*}}{k^*}A_a^{\frac{3}{2}}, \tag{49}$$

$$J^P = \frac{5}{2}^{\pm}$$

$$eg_a = \mp\frac{\sqrt{5}C}{2M_N}\left(\frac{M_{N^*}}{k^*}\right)^2 A_a^{\frac{1}{2}}, \qquad eg_a = \mp\frac{\sqrt{5}C}{2\sqrt{2}M_{N^*}}\left(\frac{M_{N^*}}{k^*}\right)^2 A_a^{\frac{3}{2}}, \tag{50}$$

$$J^P = \frac{7}{2}^{\pm}$$

$$eg_a = \pm\frac{\sqrt{35}C}{4M_N}\left(\frac{M_{N^*}}{k^*}\right)^3 A_a^{\frac{1}{2}}, \qquad eg_a = \pm\frac{\sqrt{21}C}{4M_{N^*}}\left(\frac{M_{N^*}}{k^*}\right)^3 A_a^{\frac{3}{2}}, \tag{51}$$

The above equations lead to the relations: $A^{3/2}/A^{1/2} = \sqrt{3}M_{N^*}/M_N$, $(\sqrt{2}M_{N^*}/M_N)$ and $(\sqrt{5}M_{N^*}/\sqrt{3}M_N)$, for the resonances with $J^P = \frac{3}{2}^{\pm}$ $(\frac{5}{2}^{\pm})$ and $(\frac{7}{2}^{\pm})$, respectively. Since this strong correlation is not observed for all resonances, we evaluate g by normalizing it to $(A_a^{1/2})^2 + (A_a^{3/2})^2$ and taking it's sign to be the sign of the dominant component. Instead of using the above two equations, we therefore calculate the coupling constants for $J = \frac{3}{2}, \frac{5}{2}$, and $\frac{7}{2}$ particles by using the following relations:

$$J^P = \frac{3}{2}^{\pm}$$

$$\begin{aligned} eg_a &= \pm S_a^{\frac{3}{2}}\frac{\sqrt{3}\,C}{2\sqrt{3M_{N^*}^2 + M_N^2}}\frac{M_{N^*}}{k^*}\left((A_a^{\frac{1}{2}})^2 + (A_a^{\frac{3}{2}})^2\right)^{\frac{1}{2}}, \\ S_a^{\frac{3}{2}} &= \mathrm{sign}(A^{\frac{1}{2}})\theta(h_a) + \mathrm{sign}(A^{\frac{3}{2}})\theta(-h_a), \qquad h_a = |A_a^{\frac{1}{2}}| - \frac{1}{\sqrt{3}}\frac{M_N}{M_{N^*}}|A_a^{\frac{3}{2}}|; \end{aligned} \tag{52}$$

$$J^P = \frac{5}{2}^{\pm}$$

$$\begin{aligned} eg_a &= \mp S_a^{\frac{5}{2}}\frac{\sqrt{5}\,C}{2\sqrt{2M_{N^*}^2 + M_N^2}}\left(\frac{M_{N^*}}{k^*}\right)^2\left((A_a^{\frac{1}{2}})^2 + (A_a^{\frac{3}{2}})^2\right)^{\frac{1}{2}}, \\ S_a^{\frac{5}{2}} &= \mathrm{sign}(A^{\frac{1}{2}})\theta(h_a) + \mathrm{sign}(A^{\frac{3}{2}})\theta(-h_a), \qquad h_a = |A_a^{\frac{1}{2}}| - \frac{1}{\sqrt{2}}\frac{M_N}{M_{N^*}}|A_a^{\frac{3}{2}}|. \end{aligned} \tag{53}$$

$$J^P = \frac{7}{2}^{\pm}$$

$$
\begin{aligned}
eg_a &= \pm S_a^{\frac{7}{2}} \frac{\sqrt{105}\, C}{4\sqrt{5M_{N^*}^2 + 3M_N^2}} \left(\frac{M_{N^*}}{k^*}\right)^2 \left((A_a^{\frac{1}{2}})^2 + (A_a^{\frac{3}{2}})^2\right)^{\frac{1}{2}} , \\
S_a^{\frac{5}{2}} &= \mathrm{sign}(A^{\frac{1}{2}})\theta(h_a) + \mathrm{sign}(A^{\frac{3}{2}})\theta(-h_a), \qquad h_a = |A_a^{\frac{1}{2}}| - \sqrt{\frac{3}{5}} \frac{M_N}{M_{N^*}} |A_a^{\frac{3}{2}}|. \quad (54)
\end{aligned}
$$

In above equations, we have defined $\theta(a) = 1, (0)$ for $a > (<) 0$ and $\mathrm{sign}(A) = A/ \mid A \mid$ denoting the sign of A. Obviously, our procedure can be used to investigate the N^* excitation in $\gamma N \rightarrow \omega N$ reaction only for the resonances with $\gamma N \rightarrow N^*$ helicity amplitudes given by PDG.

IV. RESULTS AND DISCUSSION

To perform calculations, the parameters of the $\gamma N \rightarrow \omega N$ amplitudes defined in Sections II and III must be specified. As discussed in section II, the parameters of the non-resonant amplitudes are taken from our previous study of $\gamma p \rightarrow \omega p$ reaction at higher energies [10]. We therefore only need to choose the parameters of the resonant amplitudes developed in Sec. III. These parameters are: the coupling constants $g_{\gamma N N^*}$ and $f_{\omega N N^*}$ in Eqs. (31) - (34), the cut-off parameters Λ_{N^*} for the $\gamma N N^*$ and $\omega N N^*$ form factors of the form of Eq. (10), and the off-shell parameters Z of Eq.(23) for the higher spin resonances.

The coupling constants, $g_{\gamma N N^*}$, are obtained by using the empirical helicity amplitudes listed by the Particle Data Group(PDG) [14] to evaluate Eqs. (28), (29), (47), (52) - (54). The corresponding $f_{\omega N N^*}$ constants are then obtained by using the relations (27)-(29) of the vector meson dominance model. Because of the uncertainties in the empirical helicity amplitudes, we consider two cases(models). In the model I we use the central values of PDG's helicity amplitudes $A_{p(n)}^{\frac{1}{2}}$, $A_{p(n)}^{\frac{3}{2}}$. These empirical helicity amplitudes for the considered N^*'s along with the calculated $\gamma N N^*$ and $\omega N N^*$ coupling constants are listed in Table I. Note that some high mass resonances listed by PDG are not included in Table I. These resonances can not be included in our investigation because of their $\gamma N \rightarrow N^*$ helicity amplitudes are not available. These resonances are expected to have negligible effects in the near threshold region.

Concerning the off-shell parameter Z, we take the simplest approach by setting $Z = -1/2$ such that the second term of Eq.(23) does not contribute. This is a rather arbitrary choice, but is supported by our finding that the calculated amplitude is rather insensitive to Z in a very wide range of $-5 \leq Z \leq +5$. This is due to the fact that the dominant N^* contribution comes from the s-channel diagram(Fig.1d) for which $\gamma^\alpha \Lambda_{\alpha\cdot\cdot}(p_s, M_{N^*}) \simeq 0$ for all projection operators Λ defined in Eqs.(35)-(41). As a result, the contributions from the Z-dependent terms in Eq.(23), which are proportional to $\gamma_\mu \gamma_\nu$, are very small.

With the above specifications, the only free parameters of model I are the cut-off $\Lambda_{N_i^*}$ for each of resonances. For simplicity, we assume the same cutoff for all N^*'s and set $\Lambda_{N_i^*} = \Lambda_{N^*}$. We then find that the unpolarized differential cross sections at low energies can be best described by setting Λ_{N^*}=0.7 GeV/c. The result is the solid curve shown in the left-side of Fig.2. The predicted beam asymmetry is the dashed curve in Fig.3. Obviously, the model I does not give a good account of the data displayed in Figs. 2 and 3.

The use of the central values of the empirical helicity amplitudes as input to our calculations is perhaps too restrictive. We therefore consider model II by allowing the values of γNN^* and ωNN^* coupling constants to vary within the ranges allowed by the uncertainties of the empirical helicity amplitudes. We then find that it is possible to get a good description of the existing data of both the unpolarized differential cross section at $E_\gamma = 1.23$ GeV [34] and the beam asymmetry at $E_\gamma = 1.175$ GeV [35]. The results are the solid curve in the right-hand-side of Fig.2 and the dot-dashed curve in Fig.3. The resulting parameters which are different from those of model I are listed in Table II. The cutoff used in this fit is $\Lambda_{N^*} = 0.75$ GeV/c.

In Fig. 2 we also show the contributions from the non-resonant amplitude (dot-dashed lines) and from the resonance excitation (dashed line). We see that the resonant contributions in two models have rather different t-dependent. The much larger resonant contribution in model II(right-hand-side of Fig.2 clearly is essential in obtaining the agreement with the data. The parameters of model II, listed in Table II, are very suggestive in future determination of the N^* parameters. We have also found that the dominant contribution to the non-resonant amplitude comes from the pseudoscalar exchange. This is consistent with our finding[10] in the investigation at higher energies.

More sizeable differences between the constructed two models can be seen in Fig. 3 for the beam asymmetry at $E_\gamma = 1.175$ GeV. The non-resonant amplitude alone yields zero asymmetry. The negative asymmetry is due to the interference between the non-resonant and resonant amplitudes. We find that the dominant resonant contribution in both models comes from the excitation of $F_{15}(1680)$ state. To illustrate this, we show in Fig. 4 the beam asymmetry calculated from keeping only the $F_{15}(1680)$ term in the resonant amplitude. We see that the main feature of the beam asymmetry can be obtained(dashed and dot-dashed curves) from the interference between this resonance state and the non-resonant amplitude. The next large contribution comes from the excitation of $D_{13}(1520)$, $S_{11}(1650)$ and $P_{13}(1720)$ states. Their role in determining the beam asymmetry is rather different. The $D_{13}(1520)$ resonance gives constructive interference with $F_{15}(1680)$, while the $S_{11}(1650)$, $P_{13}(1720)$ excitations interfere destructively and reduce the absolute value of asymmetry.

With the model II constructed above, we perform calculations at $E_\gamma = 1.125$, 1.175, and 1.23 GeV for future experimental tests. The predicted differential cross sections are the thick solid curves shown in Fig. 5. Here, we also show the contributions from various mechanisms illustrated in Fig.1. One can see that the contributions from the direct and crossed nucleon terms(short dashed curves) and N^* excitations(dashed curves) are instrumental in getting differential cross sections which are much flatter than those calculated from keeping only the pseudo scalar meson exchange (thin solid curves).

The predicted beam asymmetries, Σ_x, are shown in Fig. 6. The calculations keeping only the non-resonant amplitude yield almost zero asymmetries(dot-dashed curves). Inclusion of the resonance excitation results in negative asymmetry, in agreement with the data at $E_\gamma = 1.125$ and 1.175 GeV.

In Figs. 7,8 we depict the predicted target asymmetry(T_y) and recoil asymmetry(P_y). Again, one can see that resonance excitation results in large deviations from the pure non-resonant limit(dot-dashed curves).

In Fig. 9 we show our predictions for the tensor $V_{z'z'}$ asymmetry calculated in the Gottfried-Jackson system. The dot-dashed curves are calculated from keeping only the non-resonant amplitudes. Clearly, these are close to the value $1/\sqrt{2}$ of Eq.(19) due to only the pseudoscalar meson exchange. The resonance excitations enhance greatly the contribution from the longitudinally polarized outgoing ω mesons and hence bring $V_{z'z'}$ to negative values.

The predicted double beam-target asymmetry is shown in Fig. 10. Here we see even more dramatic effects due to N^* excitations. The non-resonant amplitude yields positive asymmetry. Adding the resonant contributions, the asymmetries at low E_γ become negative and have very different dependence on scattering angles.

The results presented above obviously reflect the consequences of the not-well-determined

ωNN^* coupling constants. It is therefore interesting to compare our values with those determined in the recent works by Post and Mosel [20], Lutz, Wolf and Friman [36], and Riska and Brown [19]. The form of the effective Lagrangians given in Ref.[20] can be obtained from our expressions by making the non-relativistic reductions. In this case the comparison can be made easily. For other two cases their relations with ours are not obvious because of the use of different couplings schemes. However, by making the non-relativistic reductions and keeping the leading terms which would be dominant near the ω production threshold, we can cast our Lagrangians into their forms and the comparisons of the coupling constants can then be made. The resulting relations are

$$
\begin{aligned}
f_{\omega NN^*}^{J^P=\frac{1}{2}^+} &\Rightarrow \frac{M_{N^*}}{m_\omega} f_{\omega NN^*}^{J^P=\frac{1}{2}^+} \text{(Ref.[20])}, \qquad \frac{M_{N^*}}{M_N^*+M} g_{\omega NN^*}^{J^P=\frac{1}{2}^+} \text{(Ref.[19])}, \\
f_{\omega NN^*}^{J^P=\frac{1}{2}^-} &\Rightarrow \frac{M_{N^*}}{m_\omega} f_{\omega NN^*}^{J^P=\frac{1}{2}^-} \text{(Ref.[20])}, \qquad \frac{M_{N^*}}{M_N^*-M} g_{\omega NN^*}^{J^P=\frac{1}{2}^-} \text{(Ref.[19])}, \\
&\Rightarrow \frac{M_{N^*}}{\sqrt{3}(M_N^*-M)} f_{\omega NN^*}^{J^P=\frac{1}{2}^-} \text{(Ref.[36])}, \\
f_{\omega NN^*}^{J^P=\frac{3}{2}^+} &\Rightarrow \frac{M_{N^*}}{2m_\omega} f_{\omega NN^*}^{J^P=\frac{3}{2}^+} \text{(Ref.[20])}, \qquad \frac{M_{N^*}}{M_N^*+M} g_{\omega NN^*}^{J^P=\frac{3}{2}^+} \text{(Ref.[19])}, \\
f_{\omega NN^*}^{J^P=\frac{3}{2}^-} &\Rightarrow \frac{M_{N^*}}{m_\omega} f_{\omega NN^*}^{J^P=\frac{3}{2}^-} \text{(Ref.[20])}, \qquad \frac{M_{N^*}+M_N}{4M} g_{\omega NN^*}^{J^P=\frac{3}{2}^-} \text{(Ref.[19])}, \\
&\Rightarrow \frac{M_{N^*}}{(M_N^*-M)} f_{\omega NN^*}^{J^P=\frac{3}{2}^-} \text{(Ref.[36])}, \\
f_{\omega NN^*}^{J^P=\frac{5}{2}^+} &\Rightarrow \frac{M_{N^*}^2}{m_\omega^2} f_{\omega NN^*}^{J^P=\frac{3}{2}^-} \text{(Ref.[20])}, \qquad \frac{M_{N^*}^2}{am_\omega^2} g_{\omega NN^*}^{J^P=\frac{3}{2}^-} \text{(Ref.[19])}, \\
\text{with } a^2 &\simeq 1+\frac{4M^2(M_{N^*}-M)^2}{m_\omega^4}+\frac{2M(M_{N^*}-M)^2}{m_\omega^2}+\cdots\ , \\
f_{\omega NN^*}^{J^P=\frac{5}{2}^-} &\Rightarrow \frac{M_{N^*}^2}{2m_\omega^2} g_{\omega NN^*}^{J^P=\frac{3}{2}^-} \text{(Ref.[19])},
\end{aligned}
\tag{55}
$$

where the factor a accounts the enhancement of transversely polarized ω in our model.

The comparison is given in Table III. We see that there are some reasonable agreements between the considered four approaches. On the other hand, very large differences exist in several cases. This is not surprising at this stage of development. Only the use of more experimental data, such as the spin observables discussed in this work, can improve the situation.

V. SUMMARY

In summary, we have investigated the role of nucleon resonances in ω photoproduction in the near threshold energy region by using the effective Lagrangian approach and the vector dominance model. By using the empirical helicity amplitudes of $\gamma N \rightarrow N^*$ transitions, a phenomenological model(model II) has been obtained to give a good description of the existing data of both the differential cross sections at $E_\gamma = 1.23$ GeV and the beam asymmetry at $E_\gamma = 1.125$ and 1.175 GeV. We have found that in the near threshold energy region $E\gamma \leq 1.25$ GeV, the dominant resonant contribution comes from $F_{15}(1680)$ and $D_{13}(1520)$ N^* states. The single and double polarization observables are strongly modified by the N^* excitations. It will be interesting to obtain data for testing our predictions given in Figs.(6)-(10).

To end, we emphasize that the tree-diagram calculations based on effective Lagrangian approach is known to be valid only in the energy region close to threshold. For investigating N^* effects at higher energies, it is necessary to include the initial and final state interactions. A dynamical approach, similar to what has been developed[17] for pion photoproduction, may have to be developed.

Acknowledgments

This work was supported in part by U.S. Department of Energy, Nuclear Physics Division, Contract No. W-31-109-ENG-38. A.I.T. thanks the warm hospitality of the nuclear theory group at Argonne National Laboratory.

---

[1] N. Isgur and G. Karl, Phys. Lett. **72B**, 109 (1977); Phys. Rev. D **18**, 4187 (1978); **19**, 2653 (1979); R. Koniuk and N. Isgur, *ibid.* **21**, 1868 (1980).

[2] B. Friman, H.J. Pirner, Nucl. Phys. A 617, 496 (1997).

[3] G.E. Brown, M. Rho, Phys. Rev. Lett. **66** 2720, (1991).

[4] T. Hatsuda, S.H. Lee, Phys. Rev. C 46 R34, (1992).

[5] R. Rapp, J. Wambach, Adv. Nucl. Phys. 25 (2000) 1.

[6] B. Friman and M. Soyeur, Nucl. Phys. **A600**, 477 (1996).

[7] Q. Zhao, Z. Li, and C. Bennhold, Phys. Lett. B **436**, 42 (1998); Phys. Rev. C **58**, 2393 (1998).

[8] Q. Zhao, Talk at 8th International Conference on Hadron Spectroscopy, Beijing, China, Aug. 1999, nucl-th/9909060.

[9] Q. Zhao, J.-P. Didelez, M. Guidal, and B. Saghai, Nucl. Phys. **A660**, 323 (1999).

[10] Yongseok Oh, A.Titov and T-S.H. Lee, Phys. Rev. C63, 025201 (2001).

[11] S. Capstick, Phys. Rev. D **46**, 2864 (1992).

[12] S. Capstick and W. Roberts, Phys. Rev. D **49**, 4570 (1994).

[13] S. Godfrey and N. Isgur, Phys. Rev. D **32**, 189 (1985); S. Capstick and N. Isgur, *ibid.* **34**, 2809 (1986).

[14] D.E. Groom, et al., Particle Data Group, Eur. Phys. J. C **15**, 1 (2001).

[15] F.E. Close, *An Introduction to Quark and Partons*, Academic press, London, New York, San Francisco, 1979.

[16] R.M. Davidson, N.C. Mukhopaghyay, and R.S. Wittman, Phys. Rev. D **43**, 71 (1991).

[17] T. Sato and T.-S. H. Lee, Phys. Rev. C **54**, 2660 (1996).

[18] M. Benmerrouche, N.C. Mukhopaghyay, and J.F. Zhang, Phys. Rev. D **51**, 3237 (1995).

[19] D.O. Riska, G.E. Brown, Nucl. Phys. A 679 (2001) 577.

[20] M. Post, U. Mosel, Nucl. Phys. **A 688**, 808 (2001).

[21] A. I. Titov, T.-S. H. Lee, H. Toki, and O. Streltsova, Phys. Rev. C **60**, 035205 (1999).

[22] H. Haberzettl, Phys. Rev. **C 56**, 2041 (1997); H. Haberzettl, C. Bennhold, T. Mart, T. Feuster, Phys. Rev. **C 58**, 40 (1998).

[23] R.M. Davidson, R. Workman, Phys. Rev. **C 63**, 058201 (2001); **C 63**, 025210 (2001).

[24] M. Pichowsky, Ç. Şavkli, and F. Tabakin, Phys. Rev. C **53**, 593 (1996).

[25] C. Bourelly, E. Leader, and J. Soffer, Phys. Rep. **59**, 95 (19980).

[26] M.G. Olsson and E.T. Osipovsky, Nucl. Phys. **B 87**, 399 (1975).

[27] H.F. Jones and M.D. Scadron, Ann. Phys. (N.Y.) 81,1 (1973).

[28] S. Nozawa, B. Blankleider and T.-S. H. Lee, Nucl. Phys. **A 513**, 459 (1990).

[29] C. Itzykson, J.-B. Zuber, *Quantum Field Theory*, McGraw-Hill, Inc., Singapore, 1985.

[30] H. Pilkuhn, The interaction of hadrons (North-Holland, Amsterdam, 1967).

[31] M. Post, S. Leupold, U. Mosel, Nucl. Phys. **A 689**, 753 (2001).

[32] D.M. Manley, E.M. Salesky, Phys. Rev. **D 45**, 4002 (1992).

[33] D.M. Manley, R.A. Arndt, Y. Goradia, and V.L. Teplitz, Phys. Rev. **D 30**, 904 (1984).

TABLE I: The helicity amplitudes $A^{\lambda}_{p(n)}$ and coupling constants for effective Lagrangians of Eqs. (21) - (25) for the model I. The helicity amplitude $A^{\lambda}_{p(n)}$ is given in unit of 10^{-3} GeV$^{-1/2}$. The resonance mass M_{N^*} is in unit of MeV. For the heavy resonances $F_{17}(1990)$ and $D_{13}(2080)$ we use the data of [Awajii 81] and for $G_{17}(2190)$ - the data of [Crawfold 80], listed in [14]. The resonance mass M_{N^*} is in unit of MeV. The helicity amplitude $A^{\lambda}_{p(n)}$ is given in unit of 10^{-3} GeV$^{-1/2}$.

N^*	M_{N^*}	$A_p^{1/2}$	$A_n^{1/2}$	eg_p	f_ω		
P_{11}	1440	-65 ± 4	40 ± 10	-0.117	-1.271		
S_{11}	1535	90 ± 30	-46 ± 27	-0.156	-2.144		
S_{11}	1650	53 ± 16	-15 ± 21	-0.088	-1.782		
P_{11}	1710	22 ± 16	-2 ± 14	0.015	0.323		
N^*	M_{N^*}	$A_p^{1/2}$	$A_n^{1/2}$	$A_p^{3/2}$	$A_n^{3/2}$	eg_p	f_ω
D_{13}	1520	-24 ± 9	-59 ± 9	166 ± 5	-139 ± 11	-0.389	5.70
D_{13}	1700	-18 ± 13	0 ± 50	-2 ± 20	-3 ± 40	0.04	1.164
P_{13}	1720	18 ± 30	1 ± 15	-19 ± 20	-29 ± 20	0.058	3.20
D_{13}	2080	-20 ± 8	7 ± 13	17 ± 11	-53 ± 34	0.055	2.264
D_{15}	1675	19 ± 8	-43 ± 12	15 ± 9	-58 ± 13	0.242	-13.89
F_{15}	1680	-15 ± 6	29 ± 9	133 ± 12	-33 ± 9	-1.33	-28.38
F_{17}	1990	30 ± 29	-1	86 ± 60	-178	2.85	-84.92
G_{17}	2190	-55	-42	81 ± 12	-126 ± 9	2.74	84.23

[34] F. J. Klein, Ph.D. thesis, Bonn Univ. (1996); SAPHIR Collaboration, F. J. Klein *et al.*, πN Newslett. **14**, 141 (1998).

[35] J. Ajaka et al., Proc. 14 Intern. Spin Physics Symposium. AIP Conference Proceedings. V 570, p. 198. Melville, NY, 2001.

[36] M. F. M. Lutz, Gy. Wolf and B. Friman nucl-th/0112052.

TABLE II: The helicity amplitudes A^{λ} and coupling constants for the model II which values are different from the corresponding values listed in the Table I. Notation is the same as in Table I.

N^*	M_{N^*}	$A_p^{1/2}$	$A_n^{1/2}$	eg_p	f_ω		
S_{11}	1650	37	−36	−0.062	−0.047		
N^*	M_{N^*}	$A_p^{1/2}$	$A_n^{1/2}$	$A_p^{3/2}$	$A_n^{3/2}$	eg_p	f_ω
P_{13}	1720	48	−14	−39	−49	0.117	−5.63
F_{15}	1680	−9	38	145	−24	−1.45	−34.97

TABLE III: Comparison of the absolute values of $f_{\omega NN^*}$ coupling constants in this model and the previous analysis by Riska and Brown [19], Post and Mosel [20], Luts, Wolf and Friman [36].

	$N^*(1440)$	$N^*(1520)$	$N^*(1535)$	$N^*(1650)$	$N^*(1680)$	$N^*(1675)$	$N^*(1700)$	$N^*(1710)$	$N^*(1720)$
this work	1.27	5.70	2.14	0.047	34.97	13.89	1.16	0.323	5.63
[19]	3.33	5.04	11.57	5.1	29.5	21.56	1.69	–	1.74
[20]	1.6 ± 0.9	6.6 ± 1.7	1.5 ± 2.4	2.4 ± 2.3	30.1 ± 6.9	–	0.4 ± 2.2	0.44 ± 2.23	1.97 ± 3.5
[36]	–	11.4	2.8	2.9	–	–	–	–	–

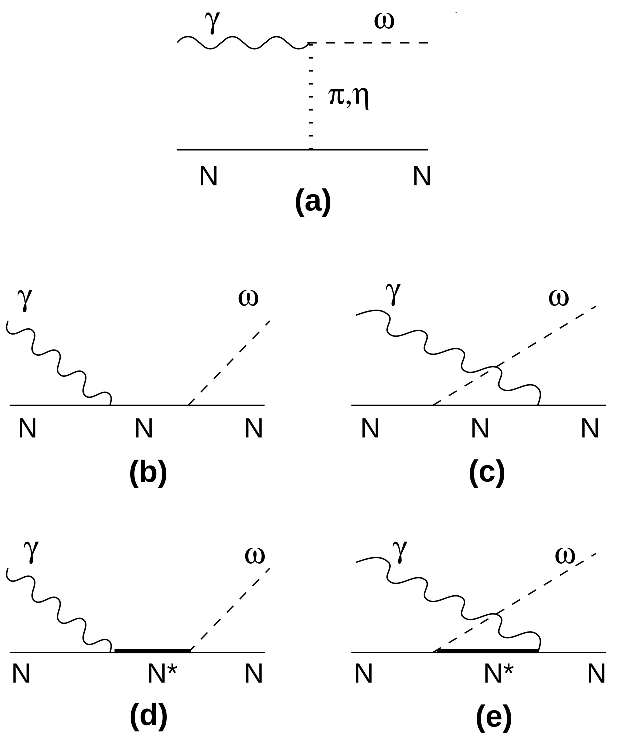

FIG. 1: Diagrammatic representation of ω photoproduction mechanisms: (a) (π, η) exchange, (b,c) direct and crossed nucleon terms, (d,e) direct and crossed resonant terms.

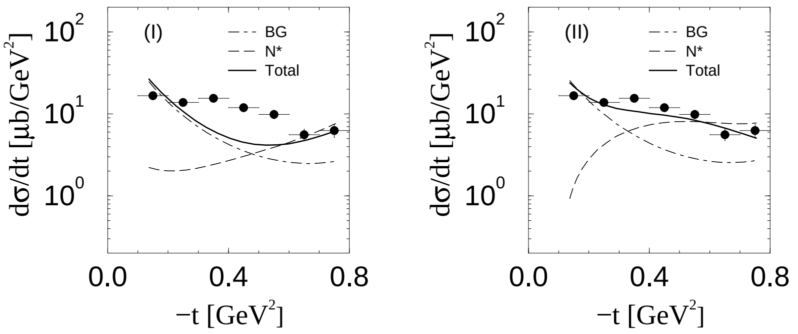

FIG. 2: Differential cross sections for $\gamma p \rightarrow p\omega$ reaction as a function of t at $E_\gamma = 1.23$ GeV for the models I (left panel), and II (right panel). The results are non-resonant channel (dot-dashed), resonance excitation (dashed), and the full amplitude (solid). Data are taken from Ref. [34].

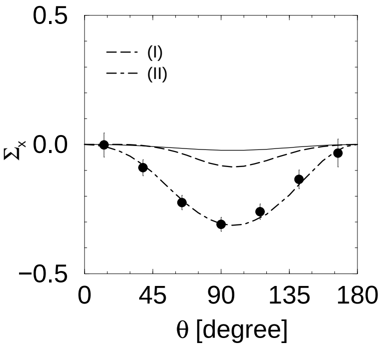

FIG. 3: Beam asymmetry as a function of $\omega-$meson production angle at $E_\gamma = 1.175$ GeV for the two models. The thin solid line is the beam asymmetry for the non-resonant background, taken separately. Data are taken from Ref. [35]

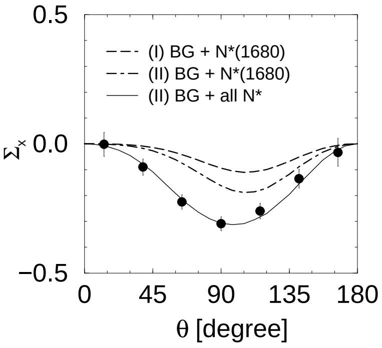

FIG. 4: Beam asymmetry as a function of ω production angle at $E_\gamma = 1.175$ GeV for the three models for the coherent sum of non-resonant background and only $F_{\frac{5}{2}^+}(1680)$ resonance. Notation is the same as in Fig. 3

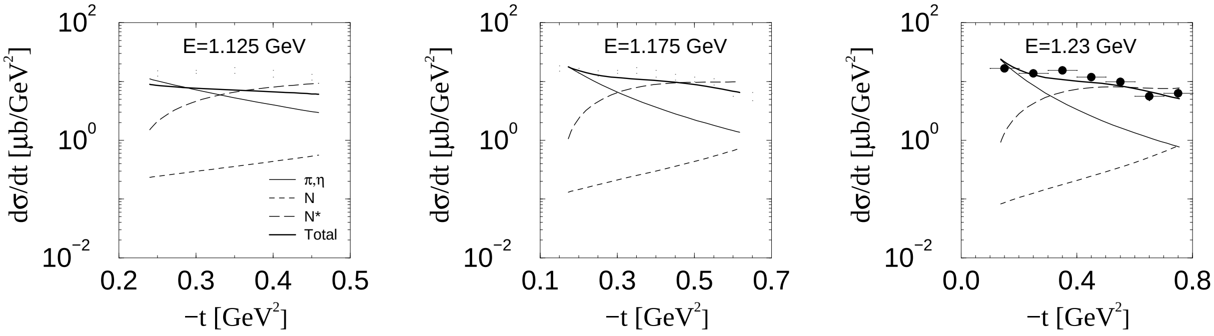

FIG. 5: Differential cross sections for $\gamma p \rightarrow p\omega$ reaction as a function of t at $E_\gamma = 1.125$, 1.175, and 1.23 GeV. The results are from pseudoscalar-meson exchange (thin solid), direct and crossed nucleon terms (short dashed), N^* excitation (dashed), and the full amplitude (thick solid). Data are taken from Ref. [34].

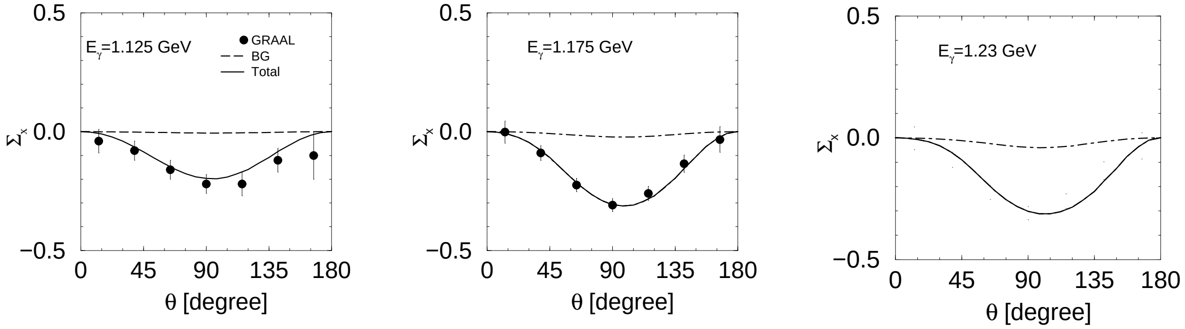

FIG. 6: Beam asymmetry at $E_\gamma = 1.125$, 1.175, and 1.23 GeV as a function of $\omega-$ production angle. The results are from the non-resonant background (BG) (dot-dashed), and the full amplitude (solid). Data are taken from Ref. [35].

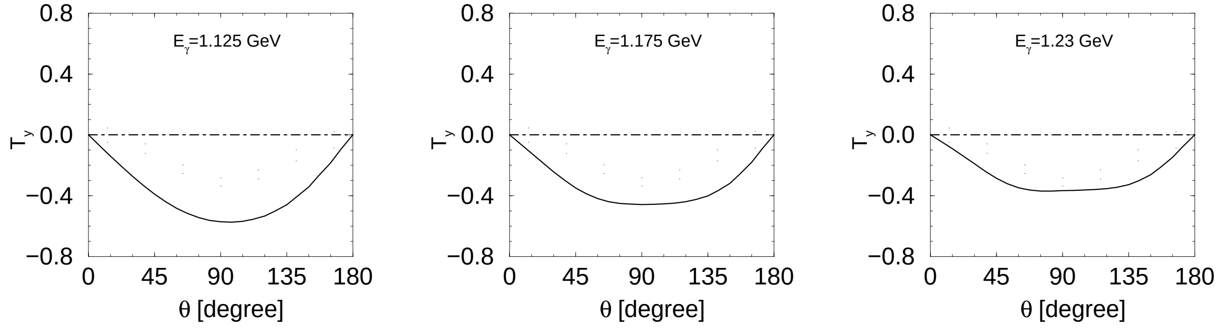

FIG. 7: Target asymmetry at $E_\gamma = 1.125$, 1.175, and 1.23 GeV as a function of $\omega-$ production angle. Notation is the same as in Fig. 6.

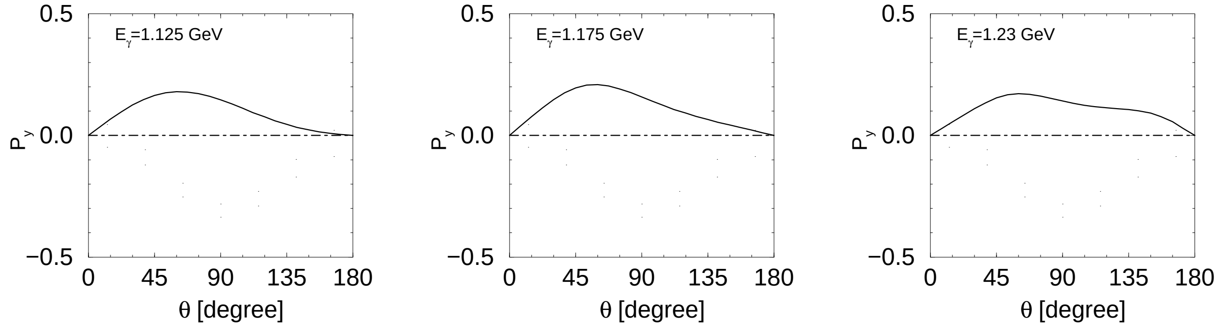

FIG. 8: Recoil asymmetry at $E_\gamma = 1.125$, 1.175, and 1.23 GeV as a function of $\omega-$ production angle. Notation is the same as in Fig. 6.

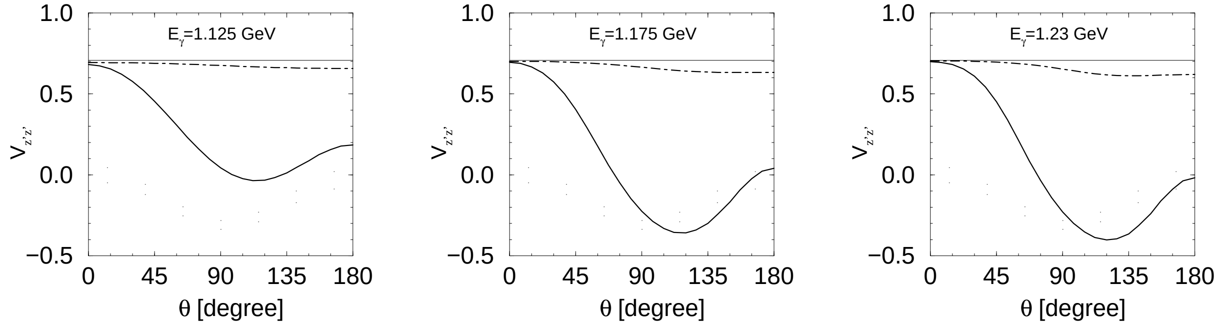

FIG. 9: The $\omega-$meson tensor asymmetry at $E_\gamma = 1.125$, 1.175, and 1.23 GeV as a function of $\omega-$ production angle. The other notation is the same as in Fig. 6.

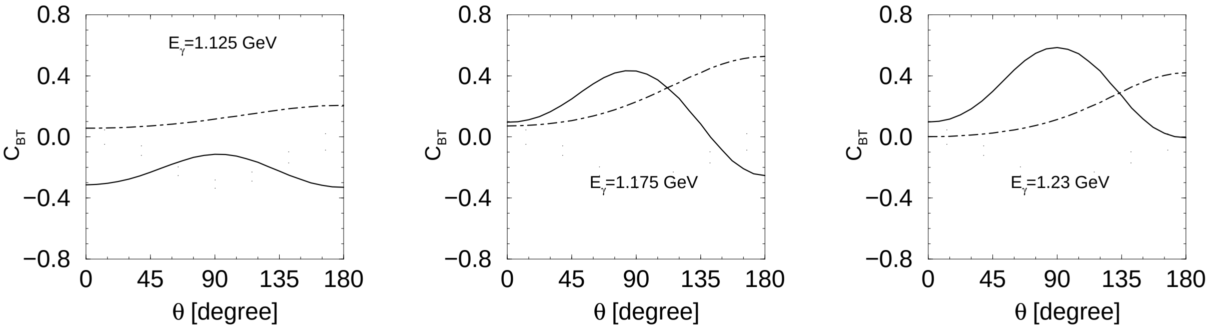

FIG. 10: Beam-target asymmetry at $E_\gamma = 1.125$, 1.175, and 1.23 GeV as a function of $\omega-$ production angle. Notation is the same as in Fig. 6.